Production of fullerenes and single-wall carbon nanotubes by high-temperature pulsed arc discharge

Toshiki Sugai, Hideki Omote, Shunji Bandow,[a] Nobuo Tanaka,[b] and Hisanori Shinohara[c]
Department of Chemistry, Nagoya University, Nagoya 464-8602, Japan

Fullerenes and single-wall carbon nanotubes (SWNTs) have been produced for the first time by the high-temperature pulsed arc-discharge technique, which has developed in this laboratory. Fullerenes are identified quantitatively by high-performance liquid chromatography (HPLC), and scanning electron microscopy (SEM) and transmission electron microscopy (TEM) observations reveal a significant amount of production of bundles of SWNTs in soot. The pulse arc production of fullerenes and SWNTs favors the high-temperature ($\geq 1000\,°C$), long pulses (≥ 1 ms) and a heavy rare gas such as Ar or Kr as a buffer gas. We have found that fullerenes and SWNTs have complementary relationships in their early stage of production. The details of the pulsed arc discharge have been obtained by observing the transition from the pulsed arc discharge to the steady arc discharge while increasing the pulse width. © *2000 American Institute of Physics.* [S0021-9606(00)71113-5]

I. INTRODUCTION

Fullerenes and single-wall carbon nanotubes (SWNTs) have so far provided new nano-scale materials in various fields. Recent progress in research on the properties of SWNTs, such as electronic[1–3] and atomic structures,[4] mechanical properties,[5] and organic functionalization,[6,7] has been outstanding, mainly due to an efficient production and purification of SWNTs. Fullerenes and related materials have been known to exhibit superconductivity,[8,9] metal encapsulation,[10,11] polymerization,[12] and various organic functionalization.[13] Fullerenes and SWNTs are produced in macroscopic quantities by the pulsed laser vaporization (laser furnace) method[14] and the electric-arc-discharge technique.[15–17] However, these methods are still far from the best methods to obtained sufficient quantities of SWNTs with high yield, high purity, and low cost. In these production methods, carbon vapors self assemble into fullerenes and SWNTs through annealing.[14–17] Several studies suggest that the ''cap structures'' of the SWNTs, which are the half spheres of fullerenes, play important roles in the formation of SWNTs.[1,18,19] There should be a close relationship in the formation process between fullerenes and SWNTs.

In an effort to elucidate the growth mechanism of fullerenes and SWNTs, we have recently developed a high-temperature pulsed arc-discharge technique[20,21] which is equipped with a dc pulsed arc-discharge mechanism inside a high temperature ($800\,°C–1200\,°C$) furnace. So far, the pulsed arc discharge has mainly been used to produce various metal[22] and carbon clusters[23] in the gas phase which were analyzed by mass spectrometry. In previous studies,[20,21] we obtained preliminary results on the production of solvent-extractable fullerenes and SWNTs by this method. One of the most important advantages of the pulsed arc discharge over the steady arc discharge is that the pulsed arc period can be varied over a wide time range ($\mu s \sim s$), which allows us to study the detailed growth processes.

Here, we present the first successful report on the production of fullerenes and SWNTs via the high-temperature pulsed arc-discharge technique. We have found that fullerenes and SWNTs have been synthesized by the pulsed arc method, incorporating Ni/Co and Ni/Y–graphite composite rods as discharge electrodes. The results have shown that both materials have close relationships in their production processes.

We have found that the yield of SWNTs starts to increase, with respect to the pulse arc width, when that of fullerenes begins to decrease. Evidently the formation of SWNTs is competitive with that of fullerenes, suggesting the presence of common (unknown) ''precursors'' in their early stage of the growth. We have also revealed the mechanisms of the pulsed arc and obtained information on the transition from the pulsed arc discharge to the steady arc discharge by increasing the pulse width from 50 μs to 300 ms.

II. EXPERIMENT

The high-temperature pulsed arc-discharge apparatus[20,21] consists of a furnace (ISUZU KRO-12K), a quartz tube ($\phi 25$ mm), electric feedthroughs with insulation quartz tubes, carbon electrodes, a water cooled trap, and a homemade pulsed HV power supply (cf. Fig. 1). The electrodes were located inside the quarts tube and the furnace to produce pulsed arc discharges in high-temperature buffer gases. A buffer gas (He, Ar or Kr) was passed through the quartz tube to thermally anneal carbon clusters and particles pro-

[a]Nanotubulites Project Japan Science and Technology Corporation, Department of Physics, Meijo University Shiogamaguchi 1-501, Tenpaku-ku, Nagoya 468-8502, Japan.
[b]Department of Applied Physics, School of Engineering, Nagoya University, Nagoya 464-8603, Japan.
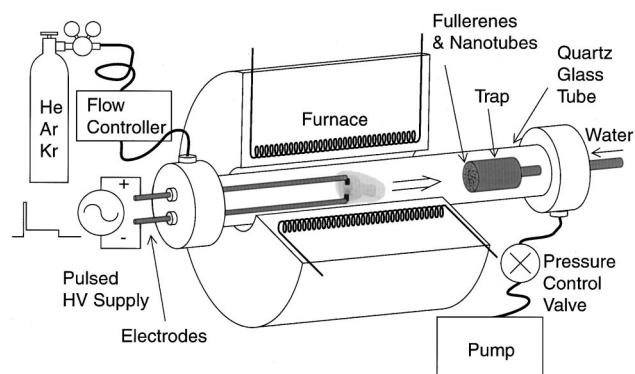[c]Author to whom correspondence should be addressed.

FIG. 1. A schematic diagram of a high-temperature pulsed arc discharge apparatus.

FIG. 2. Pulse width dependence of consumption ratios between an anode and a cathode.

duced by the pulsed arc discharge. The temperature of the tube was varied between 25 °C and 1100 °C by the furnace. The flow and pressure of the buffer gas were regulated to 300 cm^3/min and to 500 Torr, respectively.

A power supply (PS1) can provide pulsed HV voltages of typically 1.1 kV, 22 A, and 50~3000 μs duration. The repetition rate was normally 3~300 Hz with a constant duty factor (1%): The repetition rate was set, for example, to 100 Hz when the duration was 100 μs. The second power supply (PS2) was newly developed for longer pulses ~1 s and high duty factor ~10%. To achieve such a high performance, the power supply utilizes high (1.1 kV) and low (40 V) dc voltages, which were used for igniting and maintaining the discharge, respectively. The high voltage is necessary to initiate the discharge between the electrodes, but the low voltage is enough to maintain the discharge because of rapid decrease of the impedance and the voltage drop between the electrodes (cf. Sec. IV A). In contrast to the steady arc-discharge, the negative electrode was found to be consumed by the pulsed arc discharge.[20,21]

Metal doped composite graphite rods (Ni/Co: 0.7/0.7 at. %, and Ni/Y 4.2/1.0 at. %; Toyo Tanso Co. Ltd) and pure graphite rods (Toyo Tanso Co. Ltd) were cut in sizes of 10 ×5×1 mm and were used as the electrodes. The metal composite rods were produced from metal oxide, graphite powder, and a high strength pitch with high-temperature baking under 1100 °C. The fullerenes, SWNTs and other graphitic particles drifted within the tube by the gas flow and were collected on the water cooled copper trap (cf. Fig. 1).

The trapped soot was extracted by carbon disulfide and then analyzed by high-performance liquid chromatography (HPLC). The HPLC analysis was performed on a buckyprep column (nacalai tesque, ϕ4.6×250 mm) with toluene as eluent. The present HPLC system can detect fullerenes at low concentration as 100 ng/ml. The concentration of fullerenes in the soot was estimated by using HPLC peak area at 331 nm. The dependence of the fullerene concentration on temperature (25 °C to 1100 °C), HV pulse duration (50 μs to 300 ms) and buffer gas species (He, Ar, and Kr) was also measured.

The trapped soot was further characterized by scanning electron microscopy (SEM: Hitachi S-900) and transmission electron microscopy (TEM: JEOL JEM 2010) to detect
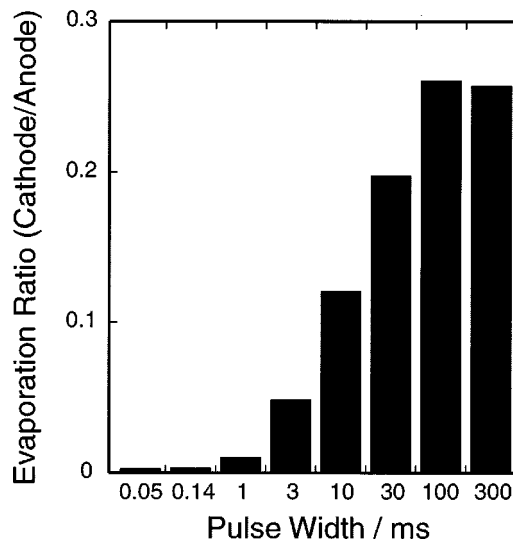
SWNTs. The TEM samples were prepared on a microscope specimen grid by a drop coating of toluene suspensions of the soot. The dependence of the production efficiencies of SWNTs on temperature (25 °C and 1000 °C), HV pulse duration (50 μs to 300 ms) and buffer gases (He, Ar, and Kr) were also studied. The production of fullerenes from Ni/Co doped graphite electrodes was also studied to obtain information on a competitive formation between fullerenes and SWNTs.

III. RESULTS

A. Evaporation profiles

Figure 2 shows the consumption ratio between the cathode and the anode of pure graphite. The ratio is around zero and only the cathode is evaporated in short pulse width range less than 1 ms. The ratio, however, starts to increase at 3 ms and keeps increasing up to 300 ms as the pulse width increases, suggesting that the anode is vaporized like the steady arc discharge. The results indicate that the transition between the pulsed arc and the steady arc occurs at 3 ms.

Figure 3 shows the vaporization profile of the pure graphite cathode. To estimate the vaporization profile ($V(t)$) on the pulse width, the differences between each adjacent data point in the sampling sequence are used as the following equation: $V(t_2) = [C(t_2) - C(t_1)]/(t_2 - t_1)$, where t_1 and t_2 are the pulse widths adjacent to each other, and $C(t_n)$ is the averaged (each pulse) vaporization consumption of the cathode at the specified pulse width of t_n. The vaporization rate steeply decreases as the discharge pulse width increases. The vaporization rate also depends on the buffer gas. The average vaporization rates at 1 ms duration are 11, 109, 169 μg/s in He, Ar, and Kr, respectively. The vaporization rate increases as the mass of the buffer gas increases.

B. Production of fullerenes via pulsed arc discharge

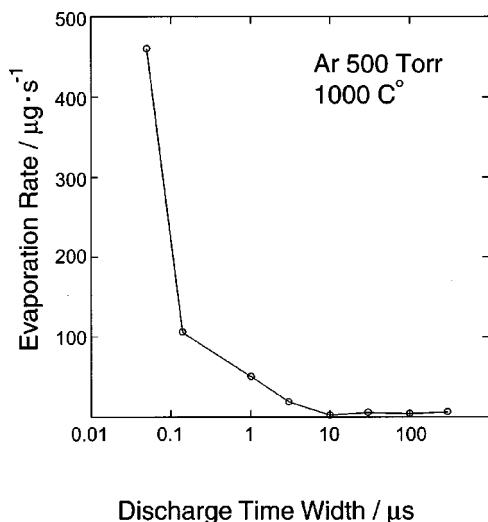Soot samples of 2–10 mg were obtained in 3–30 hours from pure carbon electrodes by the present pulsed arc dis-

FIG. 3. A vaporization profile of a negative electrode (pure graphite) against pulse width. Vaporization rate rapidly decreases with discharge time.

FIG. 5. Pulse width dependencies of C_{60} yield in soot produced by pulsed arc discharge. A distinct peak at 3 ms.

charge. Figure 4 shows HPLC chromatograms of the extracts obtained at 25 °C and 1000 °C. The HPLC peak intensity is normalized by soot weight and thus corresponds to the concentration of fullerenes in the soot. C_{60} and C_{70} are not produced at 25 °C, but are effectively produced at 1000 °C, and the fullerene yield increases as the pulse duration increases. The peaks at 3 minutes are due to the solvent. The absolute concentration of C_{60} in the soot is shown in Fig. 5. The yield of C_{60} increases until 3 ms (7.9%) as the duration increases, but decreases (1.3%) abruptly at 10 ms. The yield is relatively constant (1–2 %) up to 100 ms. At 300 ms duration, the C_{60} yield (4%) again starts to increase. The yield of C_{60} at 3 ms duration (7.9%) is comparable to those reported in

the steady arc discharge (5–20 %).[24,25] The production of higher fullerenes (C_{76}, C_{78}, and C_{84}) is more sensitive to the pulse duration than those of C_{60} and C_{70} (cf. Fig. 4).

Figure 6 shows the temperature dependence of the C_{60} production. Fullerenes are produced at higher temperatures than 800 °C. The yield of C_{60} increases as the temperature increases. Similar temperature dependencies have been reported in the laser furnace experiments.[26–28]

The C_{60} production in the high-temperature pulsed arc also depends on the buffer gas. At 1 ms pulsed discharge, the concentrations of C_{60} in the soot are 0%, 1.54%, and 1.12% in He, Ar, and Kr, respectively. Ar and Kr are much more effective than He for fullerene production.

C. Production of single-wall carbon nanotubes

SWNTs are also produced via the pulsed arc discharge from the Ni/Co doped graphite electrodes. The metal particles obviously play catalytic roles in the production of SWNTs.[15–17] Figure 7 shows TEM images of typical bundles of nanotubes which consist of individual SWNTs in the soot
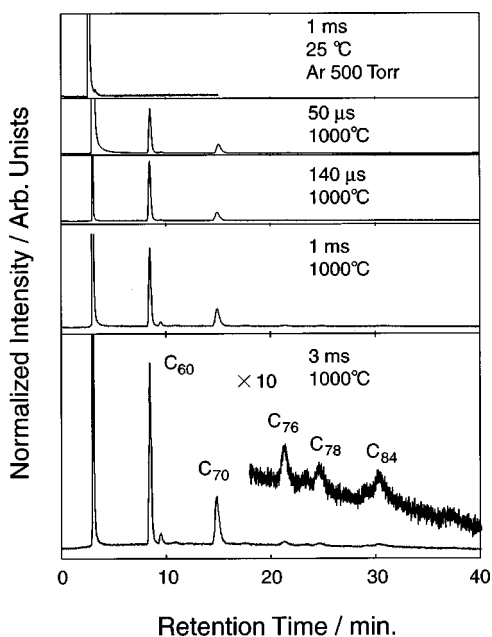

FIG. 4. HPLC chromatogram of CS_2 extracts of the soot produced by a high-temperature pulsed arc discharge. Intensities correspond to the concentration in the primary soot. Yields of fullerenes increase as the pulse width increases.
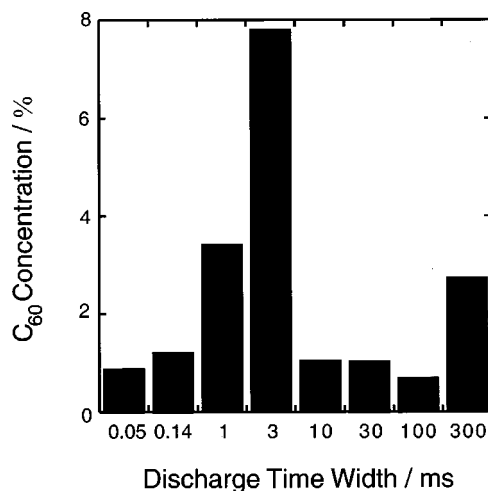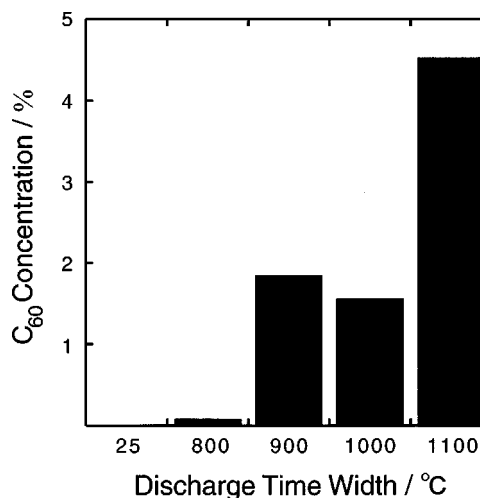

FIG. 6. Temperature dependencies of C_{60} yield in soot produced by pulsed arc discharge. The yield increases as the temperature increases.
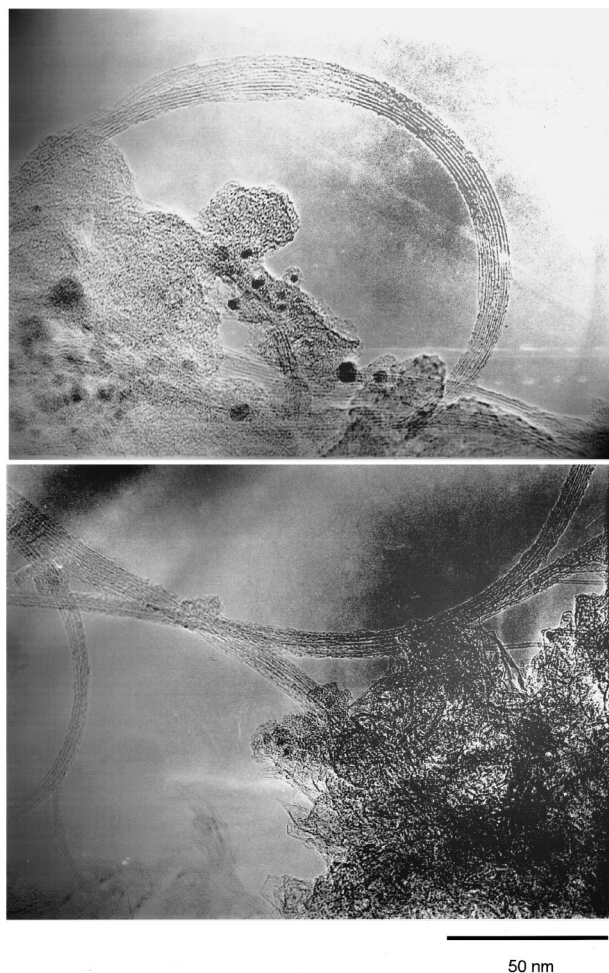
FIG. 7. TEM images of single-wall nanotubes produced with a buffer gas of Ar and a pulse width of 3 ms.

TABLE I. A summary of production efficiencies of single-wall nanotubes in various conditions. The double circles, single circles, and triangles represent high, medium, and low concentrations of the SWNTs in primary soot, respectively. The crosses indicate the absence of SWNT in the soot.

Buffer gas and temperature	Pulse width / ms								
	0.05	0.14	1	2	3	10	30	100	300
Ar 25 °C			×						
He 1000 °C			×						
Ar 1000 °C	×	×	△	○	○	○	△	○	⊙
Kr 1000 °C	△	○	○		⊙				

obtained at 2 ms pulse width with Ar buffer gas. The relative yield of the bundles of SWNTs can be evaluated by the SEM observation and is summarized in Table I. The results show that the pulse width longer than 1 ms and temperatures higher than 1000 °C are necessary to produce SWNTs. The yield increases as the pulse width increases. There is a dip of the yield of SWNTs at 30 ms, which is probably related to the transition from the pulsed arc to the steady arc (cf. Sec. III B). At 300 ms, thick tubular materials are produced (cf. Fig. 8).

The yield is also dependent on the buffer gas used. Kr is more effective than Ar for the production of SWNTs. SWNTs were not observed in a He buffer gas. Again, the temperature and buffer gas dependencies are similar to those reported in the laser furnace experiment.[27]

D. Fullerenes vs single-wall carbon nanotubes

Figure 9 shows the C_{60} yield against the pulse width produced by Ni/Co doped graphite (black bars) and pure graphite (white bars) in Ar. The yield of Ni/Co doped graphite has a maximum at 1 ms in Ar. However, the yield increases as the pulse width increases in pure graphite. In Kr, the optimum condition is obtained at 50 μs and the yield ($\sim 1\%$) is much lower than that of Ar ($\sim 3\%$). The opti-

mum conditions for C_{60} (1 ms and 50 μs) coincide with the thresholds of the production of SWNTs (see positions of the triangles in Table I). This strongly suggests that fullerenes and SWNTs have close relationships in the production processes. The C_{60} yield of Ar is higher than that of Kr, whereas Kr is much more effective to produce SWNTs than Ar.

We have also obtained much higher SWNTs yield and lower fullerenes yield by Ni/Y doped composite rods than those by Ni/Co doped composite rods. The results will be reported in a future paper.

IV. DISCUSSION

A. Mechanism of the pulsed arc discharge: an asymptote to the steady arc

In the steady arc discharge, discharge electrons are accelerated towards the anode by the applied electric field, resulting in vaporization of the anode.[24,25,29] However, the observed cathode vaporization in the pulsed arc discharge indicates a sputtering of the cathode by an ionized buffer gas such as Ar^+ or He^+ ions.

The vaporization of the negative electrode presumably takes place according to the following mechanisms.[20,21] Ar^+ or He^+ ions are produced by the discharge electrons, which are accelerated toward the negative electrode by a strong electric field between the electrodes. The accelerated ions sputter and vaporize the surface of the negative electrode.

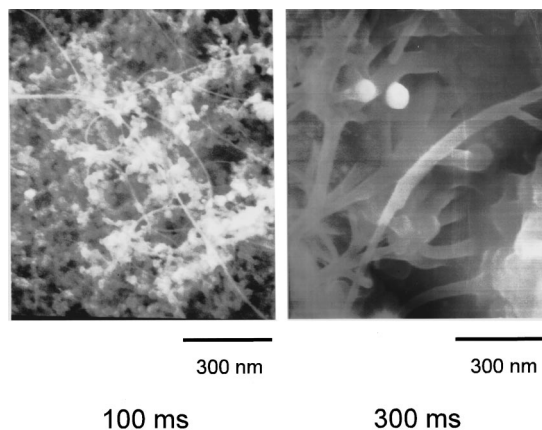100 ms   300 ms

FIG. 8. SEM images of nanotube bundles produced with a buffer gas of Ar and a pulse widths of 100 ms and 300 ms. Thick tubular materials are observed at 300 ms.
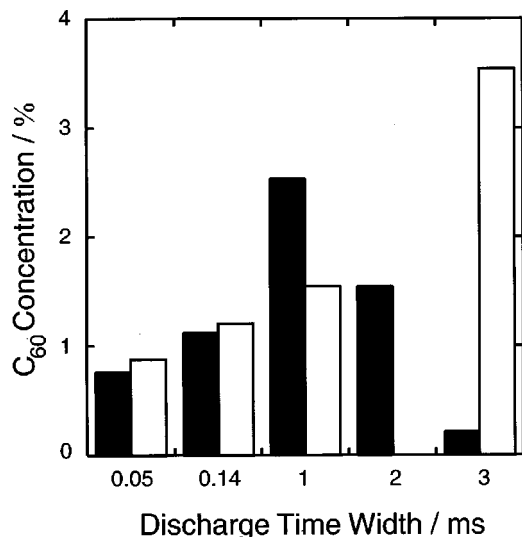
FIG. 9. Pulse width dependence of C_{60} yield produced from Ni/Co doped graphite and pure graphite in Ar 500 Torr at 1000 °C using PS1. The maximum yield is obtained at 1 ms in the case of Ni/Co doped graphite, whereas the yield of pure graphite keeps increasing as the pulse width increase.

The sputtering efficiency of Ar and Kr is much higher than that of He because of their heavier masses and lower ionization potentials.

During the vaporization, various ion species and concomitant electrons are produced in plasma, which causes a decrease of an impedance (R) between the electrodes. The impedance decrease results in a decrease of voltage drop (ΔV) between the electrodes, because ΔV is given by $\Delta V = R/(R+R_0) \cdot V_0$, where R_0 and V_0 are the output impedance and voltage of the pulsed HV power supply, respectively (50 Ω and 1.1 kV). The voltage drop (ΔV) decreases from 1.1 kV to about 20 V in about 10 μs. This results in the rapid decrease of the evaporation rate (Fig. 3) since the kinetic energy of the sputtering ions is determined by ΔV. After the rapid decrease of ΔV, the pulsed arc asymptotically approaches to the steady arc discharge with $\Delta V \approx 20$ V.[24,25] In this ''quasisteady arc discharge,'' the vaporization rate decreases gradually (cf. Fig. 3).

At pulse widths larger than 3 ms, the anode also begins to vaporize by the discharge electrons as in the steady arc discharge. This suggests that certain critical pulse widths are needed to vaporize the anode because of the smaller sputtering and heating effects of electrons than those of the buffer gas ions. This transition threshold is also supported by an experiment with a metal cathode and a graphite anode, where fullerenes are produced only from the vaporization of the anode.

Fullerenes are produced from the graphite cathode as well as the steady arc discharge, and the threshold pulse width is also 3 ms (cf. Fig. 4) because heat up and annealing of the pulsed arc become enough at 3 ms.

B. Production of fullerenes and single-wall carbon nanotubes

The observed temperature and buffer gas dependence (cf. Fig. 6, and fullerene production of Sec. III B) are similar to those of the laser furnace experiments[26–28] and are different from those of the steady arc discharge experiments.[24,25] The previous laser furnace experiments have shown that there is a threshold at about 800 °C for the production of fullerenes.[26–28] This suggests that nascent products by the laser vaporization and the pulsed arc discharge are not fullerenes; a high temperature thermal annealing is necessary to transform the nascent cluster products to fullerenes. Carbon vapors are, however, subjected to enough annealing to produce fullerenes due to the hot buffer gas heated by the steady arc discharge *per sé*. The production efficiency of fullerenes increases as the pulse width increases until 3 ms in the pulsed arc discharge. The longer pulse has a similar effect on the production of fullerenes. The annealing after carbon vaporization is also provided by the longer pulse, which is crucial to the growth of fullerenes.[20]

Bowers and co-workers have shown that cyclic ring carbon clusters are annealed into fullerenes by collision heating with a buffer gas.[30,31] The annealing effect of the high temperature buffer gas has been reported by Smalley and co-workers in the laser furnace experiments.[27] The pulsed arc-discharge experiment also shows the importance of the annealing effect due to the temperature of the buffer gas and the pulse width.

The conditions for SWNT formation are also similar to those of fullerenes produced by the pulsed arc discharge: higher temperatures and longer pulses are necessary. The temperature dependence on the SWNTs production in the pulsed arc discharge is also similar to that of the laser furnace experiments.[26–28] The longer pulse (>1 ms) and the high-temperature (>800 °C) conditions in the pulsed arc discharge can provide an efficient annealing for the carbon vapor to transform it into SWNTs.

The growth mechanism of SWNTs and the bundles has not yet fully been understood.[1,14,18,19] One of the most intriguing aspects of the SWNT growth is that the tube diameter and the corresponding bundle structure vary sensitively with metal catalysts used in the composite rods.[1,32] Obviously, metal particles/clusters play crucial roles here in the entire growth processes of SWNTs. The current pulsed arc experiments show that a certain pulse period ($1 \sim 10$ ms for Ar buffer gas) is required to obtain a sufficient amount of SWNTs in soot.

C. Correlation mechanisms between fullerenes and nanotubes

Figure 9 shows the strong correlation of production conditions between fullerenes and SWNTs when Ni/Co doped graphite is used as the electrodes. Evidently the formation of SWNTs is competitive with that of fullerenes, suggesting the presence of common ''precursors'' and common temperature and time regions in their production processes. One of the important hypotheses for the growth of SWNTs is that SWNTs come from metal/carbon fine particles.[1,18,19] The particles segregate the precursors of SWNTs from the particles during high-temperature annealing as the temperature of the particles gradually decreases. These metal/carbon fine particles seem to be the common precursors.

The vaporization profile (Fig. 3) and the yield of fullerenes (Fig. 5) suggest that carbon is not thermally vaporized like steady arc and high-temperature laser-vaporization, but is sputtered by the buffer gas ions and rapidly cooled by the buffer gas.[20,21] During these rapid vaporization and cooling processes, the vaporized carbon and metal atoms grow into amorphous carbon/metal particles, which may have weakly bound incomplete fullerene molecules.

When the pulsed arc discharge of ~1 ms, the electron and the buffer gas ions collide with the surface of the metal–carbon particles and sputter out the fullerenes. During the further discharge (1–3 ms), the inside temperature of the particles becomes high enough to be converted into SWNTs. When the particles are converted into SWNTs, the surface area of the particles abruptly increases, which may cause sudden temperature decrease of the particles and the yield of fullerenes produced from the surface. In the case of pure graphite, no SWNTs are produced. So the temperature of the carbon particles does not decrease rapidly compared with that of Ni/Co doped graphite. The yield of fullerenes, therefore, increases in longer pulsed arc (1–3 ms).

A longer discharge pulse and a Kr buffer gas have larger annealing effects on the vaporized carbonaceous materials than a shorter discharge pulse and Ar.[20,21] This suggests that fullerenes are produced in weak annealing conditions, and SWNTs tend to grow in strong annealing conditions because the size of fullerenes are much smaller than that of SWNTs. Much larger amounts of carbon atoms and annealing processes are necessary to produce SWNTs than fullerenes.

V. SUMMARY

We report the production of fullerenes and SWNTs by the high-temperature pulsed arc-discharge method, which has been newly developed in this laboratory, by using Ni/Co doped graphite and pure graphite electrodes, respectively. The mechanism of the pulsed arc has been revealed for the first time. We have found that the pulsed arc discharge evolved into the steady arc discharge at the threshold pulse width of 3 ms. The product analyses of fullerenes and SWNTs also show that the transition from the pulsed arc discharge to the steady arc discharge. The optimum conditions of fullerenes and SWNTs suggests that an apparent relationship exists in their production processes.

One of the most important advantages of the current pulsed arc method over that laser furnace technique is that the pulse width of arc discharge can be varied from ~μs to seconds via a suitable pulsed power supply, which enables us to explore the growth processes of SWNTs and fullerenes. Furthermore, the pulse arc technique can easily be combined with high vacuum systems such as time-of-flight mass spectrometer and scanning probe microscopes.

ACKNOWLEDGMENTS

[1] R. Saito, G. Dresselhaus, and M. S. Dresselhaus, *Physical Properties of Carbon Nanotubes* (Imperial College Press, London, 1998), Chap. 4.
[2] T. Odom, J. Huang, P. Kim, and C. Lieber, Nature (London) **391**, 62 (1998).
[3] M. Bockrath *et al.*, Science **275**, 1922 (1997).
[4] J. Wildoer *et al.*, Nature (London) **391**, 59 (1998).
[5] C. Cornell and L. Wille, Solid State Commun. **101**, 555 (1997).
[6] S. Wong *et al.*, Nature (London) **394**, 52 (1998).
[7] J. Chen *et al.*, Science **282**, 95 (1998).
[8] A. F. Hebard *et al.*, Nature (London) **350**, 600 (1991).
[9] K. Tanigaki *et al.*, Nature (London) **352**, 222 (1991).
[10] H. Shinohara *et al.*, Nature (London) **357**, 52 (1992).
[11] M. Takata *et al.*, Nature (London) **377**, 46 (1995).
[12] A. M. Rao *et al.*, Science **259**, 955 (1993).
[13] *The Chemistry of Fullerenes*, edited by R. Taylor (World Scientific, London, 1995).
[14] A. Thess *et al.*, Science **273**, 483 (1996).
[15] S. Iijima and T. Ichihashi, Nature (London) **363**, 603 (1993).
[16] D. S. Bethune *et al.*, Nature (London) **363**, 605 (1993).
[17] Y. Saito *et al.*, J. Phys. Chem. Solids **54**, 1849 (1993).
[18] Y. Saito, M. Okuda, M. Tomita, and T. Hayashi, Jpn. J. Appl. Phys. **33**, L526 (1994).
[19] M. Yudasaka, T. Komatsu, T. Ichihashi, and S. Iijima, J. Phys. Chem. B **102**, 4892 (1998).
[20] T. Sugai, H. Omote, and H. Shinohara, Eur. Phys. J. D **9**, 369 (1999).
[21] T. Sugai *et al.*, Jpn. J. Appl. Phys. **38**, L477 (1999).
[22] S. Hunsicker, R. O. Jones, and G. Ganteför, J. Chem. Phys. **102**, 5917 (1995).
[23] W. Lu, R. Huang, J. Ding, and S. Yang, J. Chem. Phys. **104**, 6577 (1996).
[24] Y. Saito *et al.*, Chem. Phys. Lett. **200**, 643 (1992).
[25] Y. Achiba *et al.*, Mater. Sci. Eng., B **19**, 14 (1993).
[26] R. E. Haufler *et al.*, Mater. Res. Soc. Symp. Proc. **206**, 627 (1991).
[27] T. Guo *et al.*, Chem. Phys. Lett. **243**, 49 (1995).
[28] T. Wakabayashi *et al.*, Z. Phys. D: At., Mol. Clusters **40**, 414 (1997).
[29] R. E. Haufler *et al.*, J. Phys. Chem. **94**, 8634 (1990).
[30] G. von Helden, M. T. Hsu, P. R. Kemper, and M. T. Bowers, J. Chem. Phys. **95**, 3835 (1991).
[31] G. von Helden, M. T. Hsu, N. Gotts, and M. T. Bowers, J. Phys. Chem. **97**, 8182 (1993).
[32] A. Kasuya *et al.*, Phys. Rev. Lett. **78**, 4434 (1997).